# Altered Chloroplast Development and Delayed Fruit Ripening Caused by Mutations in a Zinc Metalloprotease at the *lutescent2* Locus of Tomato[1][W][OA]

**Cornelius S. Barry*, Georgina M. Aldridge[2], Gal Herzog[3], Qian Ma, Ryan P. McQuinn, Joseph Hirschberg, and James J. Giovannoni**

Department of Horticulture, Michigan State University, East Lansing, Michigan 48824 (C.S.B., Q.M.); Boyce Thompson Institute for Plant Research, Ithaca, New York 14853 (G.M.A., R.P.M., J.J.G.); Department of Genetics, Hebrew University of Jerusalem, Jerusalem 91904, Israel (G.H., J.H.); and United States Department of Agriculture, Agricultural Research Service, Robert W. Holley Center for Agriculture and Health, Cornell University, Ithaca, New York 14853 (R.P.M., J.J.G.)

The chloroplast is the site of photosynthesis in higher plants but also functions as the center of synthesis for primary and specialized metabolites including amino acids, fatty acids, starch, and diverse isoprenoids. Mutants that disrupt aspects of chloroplast function represent valuable tools for defining structural and biochemical regulation of the chloroplast and its interplay with whole-plant structure and function. The *lutescent1* (*l1*) and *l2* mutants of tomato (*Solanum lycopersicum*) possess a range of chlorophyll-deficient phenotypes including reduced rates of chlorophyll synthesis during deetiolation and enhanced rates of chlorophyll loss in leaves and fruits as they age, particularly in response to high-light stress and darkness. In addition, the onset of fruit ripening is delayed in *lutescent* mutants by approximately 1 week although once ripening is initiated they ripen at a normal rate and accumulation of carotenoids is not impaired. The *l2* locus was mapped to the long arm of chromosome 10 and positional cloning revealed the existence of a premature stop codon in a chloroplast-targeted zinc metalloprotease of the M50 family that is homologous to the Arabidopsis (*Arabidopsis thaliana*) gene *ETHYLENE-DEPENDENT GRAVITROPISM DEFICIENT AND YELLOW-GREEN1*. Screening of tomato germplasm identified two additional *l2* mutant alleles. This study suggests a role for the chloroplast in mediating the onset of fruit ripening in tomato and indicates that chromoplast development in fruit does not depend on functional chloroplasts.

The chloroplast is a defining organelle of plant cells, serving as the site of the biochemical reactions associated with photosynthesis as well as the synthesis of amino acids, fatty acids, carotenoids, vitamins, and a range of specialized metabolites (Armbruster et al., 2011). The chloroplast is derived from an ancient cyanobacterial endosymbiont with many of the ancestral genes of this organism incorporated into the host genome (Timmis et al., 2004). Current estimates suggest that there are between 2,000 and 3,000 chloroplast-localized proteins, the vast majority of which are encoded by the host genome (Armbruster et al., 2011). Therefore, chloroplast homeostasis requires coordination of the nuclear and plastid genomes together with the transport of these nuclear-encoded proteins into the chloroplast, their processing, folding, and assembly into functional protein complexes and their subsequent degradation. These processes must be intricately regulated to reflect changes in plastid function during development, the metabolic status of the cell, and be responsive to environmental conditions that perturb chloroplast function. Developing a systematic understanding of the function of chloroplast-localized proteins has broad implications for defining and manipulating plant metabolism and considerable progress has been made in this area, particularly in model organisms (Waters and Langdale, 2009; Ajjawi et al., 2010; Armbruster et al., 2011). Investigating the function of chloroplast-localized proteins in diverse species with novel physiology or specialized metabolism will provide additional and important insight into the functions of this unique organelle.

The onset of fruit ripening is marked by a reprogramming of cellular metabolism that often includes cell wall modifications together with associated fruit

[1] This work was supported by startup funds from Michigan State University and Michigan AgBioResearch (to C.S.B.), the National Science Foundation Plant Genome Program (grant nos. IOS–0923312 and DBI0606595 to J.J.G.), the Israel Science Foundation (grant nos. 1685/09 and EU–FP7 METAPRO 244348 to J.H.), and a Hughes Undergraduate Research Fellowship (to G.M.A.).

[2] Present address: Beckman Institute, University of Illinois, Urbana, IL 61801.

[3] Present address: Department of Molecular Microbiology and Biotechnology, Tel-Aviv University, Tel-Aviv 69978, Israel.

* Corresponding author; e-mail barrycs@msu.edu.

The author responsible for distribution of materials integral to the findings presented in this article in accordance with the policy described in the Instructions for Authors (www.plantphysiol.org) is: Cornelius S. Barry (barrycs@msu.edu).

[W] The online version of this article contains Web-only data.

[OA] Open Access articles can be viewed online without a subscription.

www.plantphysiol.org/cgi/doi/10.1104/pp.112.197483

 

softening, the conversion of chloroplasts into chromoplasts and the synthesis of brightly colored pigments such as carotenoids, the conversion of starch into simple sugars, and the synthesis of volatile compounds that influence taste and aroma. These biochemical processes are highly regulated and contribute to the transformation of the fruit from an unpalatable and often toxic organ into one that is attractive and nutritious for seed-dispersing fauna (Barry, 2010; Klee and Giovannoni, 2011). The factors that regulate the ripening transition are not fully understood, although specific transcription factors belonging to the MADS-box and SQUAMOSA PROMOTER BINDING PROTEIN families are necessary for ripening and affect multiple aspects of the ripening process, including ethylene synthesis, softening, color change, and aroma volatile production (Herner and Sink, 1973; Sink et al., 1974; Vrebalov et al., 2002, 2009; Manning et al., 2006; Itkin et al., 2009; Kovács et al., 2009; Chung et al., 2010; Jaakola et al., 2010; Karlova et al., 2011; Martel et al., 2011; Seymour et al., 2011; Lee et al., 2012). In climacteric fruit such as tomato (*Solanum lycopersicum*), these transcription factors act upstream of ethylene biosynthesis and ethylene is required for full development of the ripe phenotype (Barry and Giovannoni, 2007; Klee and Giovannoni, 2011; Martel et al., 2011). However, recent research has also implicated additional hormones in mediating the onset of fruit ripening, including brassinosteroids and abscisic acid (Nakano et al., 2003; Lisso et al., 2006; Symons et al., 2006; Zhang et al., 2009; Chai et al., 2011; Jia et al., 2011). Together, these data suggest a complex interplay of transcriptional regulation and hormonal signals influence the ripening of fleshy fruits.

The chloroplast and subsequent development of the carotenoid-rich chromoplast in ripening fruits greatly impacts overall fruit quality with plastid-derived primary and secondary metabolites influencing multiple aspects of the ripe phenotype, including nutrient content, color, and aroma (Klee, 2010). Consequently, many of the enzymes involved in these ripening-induced metabolic changes are localized or associated with either the chloroplast or the chromoplast (Chen et al., 2004; Klee, 2010). Additionally, several mutants that alter different aspects of fruit quality do so through changes in either chloroplast or chromoplast biochemistry. For example, the *high-pigment1* (*hp-1*), *hp-2*, and *hp-3* loci possess altered chloroplast number and ultrastructure, contributing to fruits with elevated levels of chlorophyll, carotenoids, and flavonoids, together with altered patterns of aroma volatile production (Yen et al., 1997; Bino et al., 2005; Kolotilin et al., 2007; Galpaz et al., 2008; Kovács et al., 2009). Similarly, inhibition of chlorophyll degradation due to mutations in tomato and pepper (*Capsicum annuum*) homologs of the chloroplast-targeted STAY-GREEN protein of rice (*Oryza sativa*), are responsible for the *green-flesh* and *chlorophyll retainer* mutations of tomato and pepper that influence fruit color (Barry et al., 2008; Borovsky and Paran, 2008). Recently, multiple aspects of the ripening process, including the ethylene climacteric and carotenogenesis, were found to be disrupted in the *Orange ripening* ($Orr^{DS}$) mutant that encodes the M subunit of the plastidial NADH dehydrogenase complex (Nashilevitz et al., 2010). These studies illustrate the important role of the chloroplast in influencing fruit ripening and the quality of fleshy fruit.

The *lutescent* mutants of tomato, *lutescent1* (*l1*) and *l2*, are nonallelic monogenic mutants that have identical phenotypes resulting in an early and progressive loss of chlorophyll from leaves and fruits. In fruit tissue, the loss of chlorophyll during development renders the fruit a whitish-yellow color prior to the onset of ripening (Kerr, 1956). Here we report that *l1* and *l2* mutants exhibit pleiotropic chlorophyll-deficient phenotypes including hypersensitivity to high-light stress and delayed deetiolation. In addition, mutation at the *l1* and *l2* loci leads to a delay in the onset of fruit ripening, suggesting the possibility of a chloroplast-derived signal that stimulates fruit ripening. Concomitant with the diverse chlorophyll-deficient phenotypes, positional cloning of the *l2* locus revealed the presence of a point mutation that introduces a premature stop codon in a tomato homolog of *ETHYLENE-DEPENDENT GRAVITROPISM DEFICIENT AND YELLOW-GREEN1* (*EGY1*), which encodes a chloroplast-targeted zinc metalloprotease required for chloroplast development in Arabidopsis (*Arabidopsis thaliana*; Chen et al., 2005).

## RESULTS

### *lutescent* Mutants Display Pleiotropic Chlorophyll-Deficient Phenotypes

Developing fruits of the *l1* and *l2* mutants of tomato are characterized by reduced chlorophyll content, leading to mature fruits that are whitish yellow rather than the typical green color associated with wild-type Ailsa Craig (AC) fruit (Fig. 1A). At the cellular level mature green AC fruits viewed using confocal laser-scanning microscopy show significant amounts of chlorophyll autofluorescence and this is almost completely absent in mature fruits of *l1* and *l2* mutants (Fig. 1B). The chlorophyll loss observed in *l1* and *l2* fruits is progressive with increasing age but the average chloroplast number per cell in young developing fruits at 20 d post anthesis was considerably lower in *l1* and *l2* compared to AC (Fig. 1C). Growing *l1* and *l2* mutants over several years it was noted that the chlorophyll loss in fruits is typically more exaggerated in plants grown during the summer when light intensities are higher and photoperiods longer and was often accompanied by accumulation of purplish epidermal pigments that are likely to be anthocyanins (Fig. 1D). A lack of chlorophyll accumulation is also observed in developing pistils of *l1* and *l2* flowers (Fig. 1E). Progressive and early chlorophyll loss is also a feature of the leaves of *l1* and *l2* (Fig. 1F). This phenomenon is exaggerated in plants grown under high-light conditions where substantial chlorophyll loss was

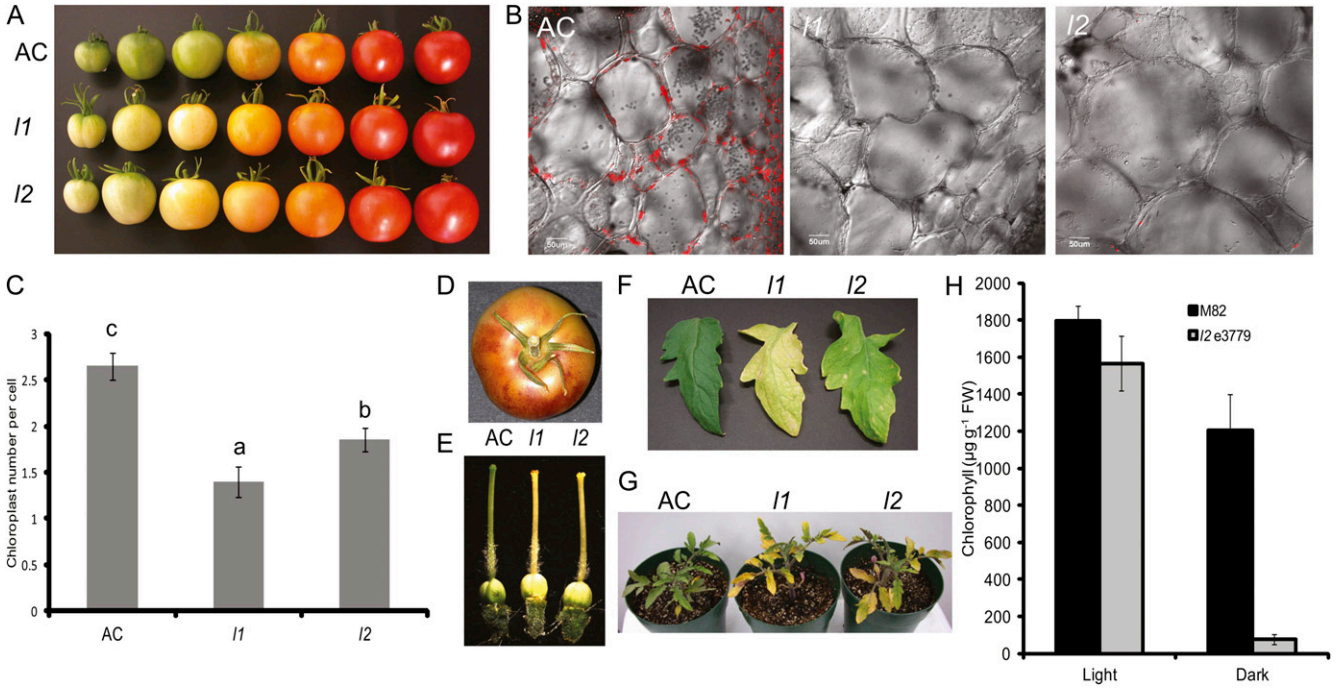


**Figure 1.** Phenotypes of the *lutescent* mutants. A, Phenotypes of developing and ripening fruit of *l1* and *l2* mutants compared to wild-type (AC) fruit. B, Confocal laser-scanning microscopy images of AC, *l1*, and *l2* fruits at the mature stage of development showing chlorophyll autofluorescence. C, Chloroplast number per cell in immature green fruit pericarp at 20 d post anthesis. Data are presented as the mean ± SE of at least 103 cells. Means followed by different letters indicate statistical significance at $\alpha = 0.05$. D, Image of a mature *l1* fruit displaying elevated anthocyanin accumulation in the fruit peel. E, Chlorophyll-deficient phenotypes in the pistils of *l1* and *l2*. F, Fully expanded leaflets of AC, *l1*, and *l2* highlighting increased susceptibility to chlorophyll loss in each mutant. G, Phenotype of 3-week-old AC, *l1*, and *l2* plants grown under high-light conditions. H, Chlorophyll breakdown in the dark in leaves of *l2* e3779. Chlorophyll concentration was determined in leaves of plants of mutant *l2* e3779 and its isogenic wild-type cv M82 grown for either 7 weeks in the light or 5 weeks in the light followed by 14 d under complete darkness. Data are presented as the mean ± SE ($n = 6$).

observed even in young expanding leaves but is also apparent in *l2* plants held in the dark for 2 weeks (Fig. 1, G and H). Leaves of a second *l2* mutant allele, designated *l2* 3779, which was identified in an ethane methylsulfonate (EMS) mutant screen in the M82 cultivar (Menda et al., 2004; see below for details of this allele) had 13% less chlorophyll than leaves of wild-type cv M82 when grown under light conditions. However, following 2 weeks in darkness, *l2* e3779 lost 95% of the chlorophyll content whereas M82 leaves lost only 37% (Fig. 1H).

### *lutescent* Mutants Exhibit Reduced Rates of Deetiolation and Thylakoid Membrane Formation

The conversion of etioplasts into chloroplasts and the subsequent development of photosynthetic competency is regulated by light (Fankhauser and Chory, 1997). To establish whether the *l1* and *l2* loci impact photomorphogenesis, the rate of deetiolation was determined in the cotyledons of dark-grown seedlings exposed to light. Dark-grown seedlings of *l1* and *l2* displayed the typical etiolated phenotype observed in AC seedlings (data not shown). However, upon exposure to light, a delay in chlorophyll accumulation was observed in both mutants (Fig. 2A). Cotyledons of wild-type AC seedlings initiated chlorophyll synthesis within 2 h of transfer to the light and this steadily increased over the 24 h time frame of the experiment. In contrast, both *l1* and *l2* accumulated chlorophyll at a slower rate and achieved less than 60% of the levels attained by AC seedlings after 24 h of light exposure. Concomitant with the reduced rates of chlorophyll accumulation during deetiolation, examination of plastid ultrastructure revealed impaired development of the thylakoid membranes in the chloroplasts of *l1* and *l2* mutants compared to those of AC plastids (Fig. 2B). Although chlorophyll accumulates more slowly during deetiolation, the chlorophyll content of fully expanded leaves is similar in AC, *l1*, and *l2* before the onset of early chlorophyll loss (Fig. 2C).

### Photosynthesis and Yield in *lutescent* Fruit

Developing tomato fruit are green due to the presence of chloroplasts that are mainly localized in the outer pericarp wall. Chlorophyll concentration in the outer pericarp tissue of fruit of cv M82 varies between fruit and with the stage of development and on

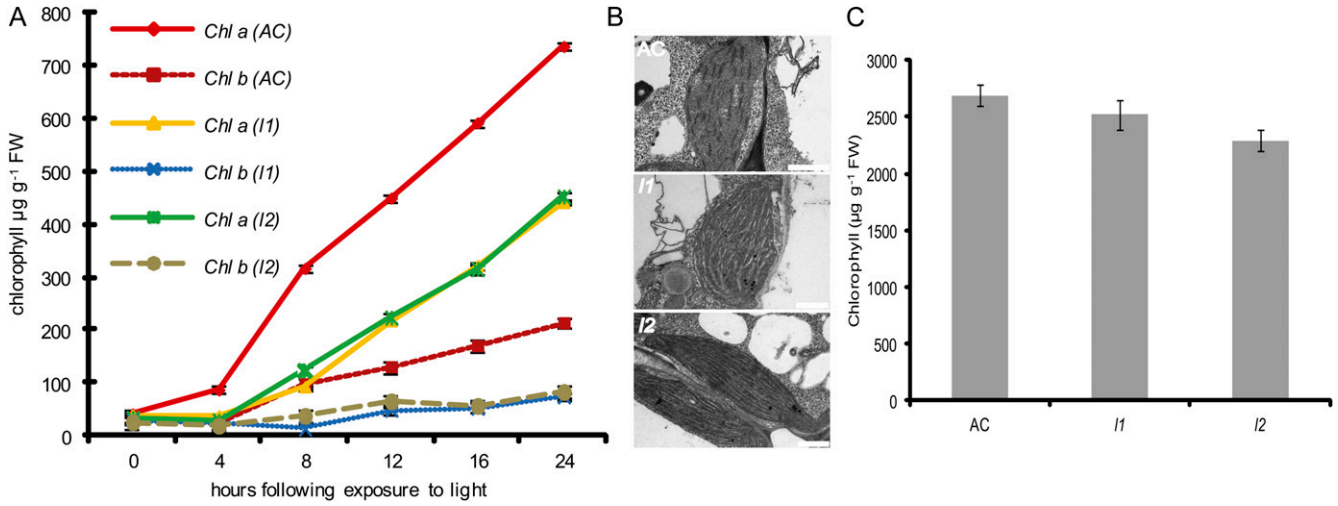


**Figure 2.** Inhibition of photomorphogenesis in *lutescent* mutants. A, Chlorophyll *a* (Chl *a*) and chlorophyll *b* (Chl *b*) levels in cotyledons of dark-grown seedlings following exposure to light. Data are presented as the mean of 10 replicates per data point ± SE. B, Transmission electron micrographs of developing chloroplasts of cotyledons following 24 h of light exposure. Scale bars are equivalent to 1 $\mu$m. C, Chlorophyll content in expanded leaves of *lutescent* mutants. Data are presented as the mean of eight replicates per data point ± SE.

average is 50- to 100-fold lower than in leaves (data not shown). The photosynthetic activity of M82 and *l2* e3779 fruit at the mature green stage of development was determined by chlorophyll fluorescence (Fig. 3A). The concentration of chlorophyll was 22.2 ± 1.2 $\mu$g g$^{-1}$ fresh weight in M82 and 2.8 ± 0.3 $\mu$g g$^{-1}$ fresh weight in *l2* e3779. PSII efficiency in fruit of M82 was similar to that of leaves (data not shown). In contrast, the fluorescence level of *l2* e3779 fruit was lower than in M82 and the efficiency of PSII was significantly impaired (Fig. 3A). The determinate growth habit of the M82 variety enables quantitative analysis of fruit yield and overall biomass during harvesting. Plants of M82 and *l2* 3779 were grown in the field during April to July, 2011. Individual plants were analyzed at time of harvesting with the *l2* 3779 mutant exhibiting a 17% lower yield and biomass production than M82 (Fig. 3B).

### The Onset of Fruit Ripening Is Delayed in *lutescent* Mutants

Together with the altered chlorophyll content in the fruits of the *lutescent* mutants (Fig. 1, A and B), it was observed that fruits of each mutant ripened slightly, but consistently, later than AC fruit. This was confirmed through determining the duration from anthesis to the onset of ripening (breaker stage) that revealed an approximate delay of 6 d in the mutants compared with wild type (Fig. 4A). This delay in the onset of ripening was also observed in detached fruits harvested at the mature green stage of development and allowed to ripen off the vine. The onset of ethylene synthesis in detached fruits was delayed in both *l1* and *l2* and failed to reach the same levels as that observed in AC fruits (Fig. 4B). This slow-ripening phenotype appeared to be specific to a delay in the onset of the ripening process as once ripening was initiated the rate of progression appeared identical in wild-type and mutant plants with lycopene accumulation progressing at the same rate with both mutant and wild-type fruits becoming fully ripe at approximately 7 d after the onset of ripening (Supplemental Fig. S1). Furthermore, ethylene treatment of wild-type AC, *l1*, and *l2* fruits at the mature green stage of development led to the onset of ripening within 2 d of treatment in each genotype, indicating that ethylene responsiveness is not significantly altered in mutant fruits (Supplemental Fig. S2). Similarly, the ethylene responsiveness of *l1* and *l2* dark-grown seedlings was normal (Supplemental Fig. S2). Together, these data suggest that mature green *l1* and *l2* fruit are fully competent to ripen yet are perturbed in a signal that initiates ethylene synthesis and therefore the onset of fruit ripening.

### Positional Cloning of the *l2* Locus

Classical linkage mapping indicated that the *l2* mutant mapped in close proximity to the *tangerine* and *hairs absent* loci on linkage group VII that was subsequently identified as the long arm of chromosome 10 (Kerr, 1956). Using an F2 population of 60 individuals derived from an interspecific cross *l2*/*l2* (tomato) × *L2*/*L2* (*Solanum galapagense*), the *l2* locus was mapped to a 7.5 centimorgan (cM) region of the long arm of chromosome 10 between the flanking RFLP markers T1682 and T802 (data not shown). Upon increasing the size of the F2 mapping population to 799 individuals by screening for recombinant individuals between T1682 and T0802 the position of the *L2* locus was refined to a 0.88 cM interval between the RFLP markers

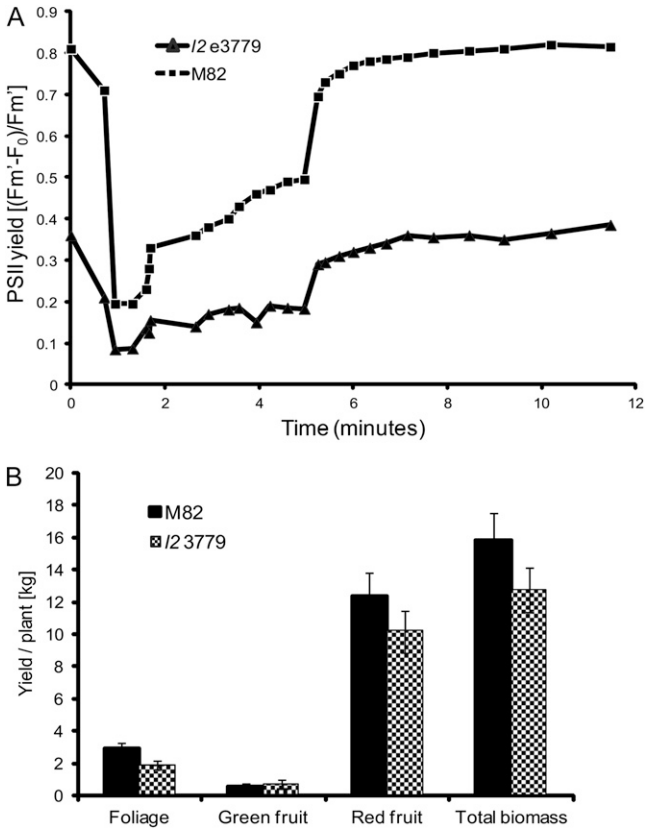


**Figure 3.** Photosynthesis and yield in *l2* e3779. A, Efficiency of PSII activity was determined by fluorescence measurements in fruit of *l2* e3779 and M82. B, Total yield and biomass of field-grown plants of *l2* e3779 and M82 (kg/plant). Data are presented as the mean of 11 replicates per data point ± SE.

T0615 and T0736 (Fig. 5A). T0615 and T0736 were used to screen three high $M_r$ tomato genomic DNA libraries made from DNA extracted from *Solanum pennellii* and *S. galapagense* (Li et al., 2005; Chen et al., 2007). Five individual clones were found to hybridize to T0615 and a single 140-kb clone, 31F20, was isolated following screening with T0736. The ends of these clones were isolated by direct DNA sequencing and specific primers were designed to amplify each end by PCR. These ends were converted to RFLP probes to enhance the resolution of the genetic map and to position the genomic clones relative to one another. A probe derived from the reverse end of 31F20 (31R) hybridized to clone 178I9, indicating that the *L2* locus was contained on two overlapping clones at a maximum physical distance of approximately 200 kb. 31R was used as a probe to screen a tomato cosmid library and a single clone, LeCOS196E17, was identified. The ends of this clone were isolated as previously described and converted to RFLP markers. Genetic mapping indicated that the *l2* locus lies within clone LeCOS196E17, 0.06 cM from 196R and 0.19 cM from 196F. LeCOS196E17 was sequenced revealing five predicted genes, corresponding to the tomato genome locus identifiers *Solyc10g081450* through *Solyc10g081490* (SL2.40Ch10:61831485–61868274). Sequence similarity searches with each predicted gene revealed that *Solyc10g081450* encodes an $\alpha/\beta$-fold hydrolase-related protein, *Solyc10g081460* encodes a predicted amino acid transporter, *Solyc10g081470* encodes a chloroplast-targeted zinc metalloprotease, *Solyc10g081480* encodes a protein of unknown function, and *Solyc10g081490* encodes a MYB transcription factor. Fragments of each gene were converted into RFLP markers and were mapped in the F2 population. *Solyc10g081470* cosegregated with the mutant phenotype whereas *Solyc10g081480* and *Solyc10g081460* were 0.06 and 0.13 cM from the *L2* locus, respectively, suggesting that *Solyc10g081470* is the candidate gene for the *l2* locus.

Sequencing of the predicted full-length cDNA of *Solyc10g081470* amplified by reverse transcription (RT)-PCR from *L2*/*L2* and *l2*/*l2* genotypes revealed a single T → A substitution at base 1574 of the cDNA clone (exon 10 in the genomic clone) in the *l2* mutant. The substitution results in the conversion of Leu 525 into a stop codon, truncating the predicted protein by 23 amino acids. Confirmation that the single base pair substitution in *Solyc10g081470* is the underlying cause of the *l2* mutant phenotype was achieved through complementation analysis. The full-length

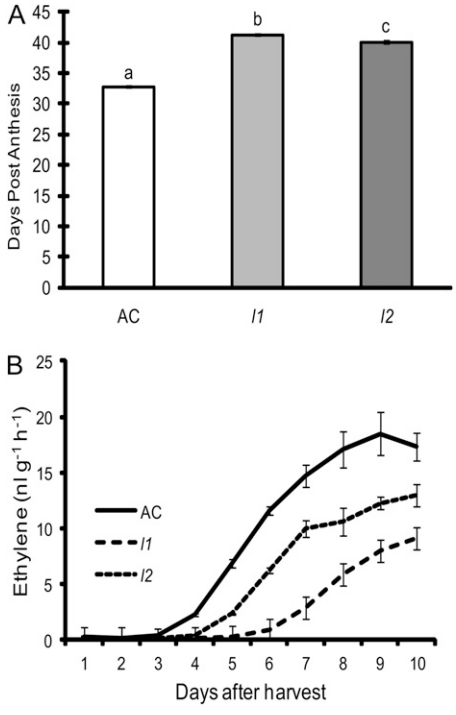


**Figure 4.** The onset of fruit ripening is delayed in *lutescent* mutants. A, The number of days from anthesis to the onset of ripening was determined for each genotype. Data are presented as the mean of 71 replicates per data point ± SE. Means followed by different letters indicate statistical significance at $\alpha = 0.001$. B, Ethylene synthesis in detached fruits of AC, *l1*, and *l2*. Data are presented as the mean of three replicates per data point ± SE.

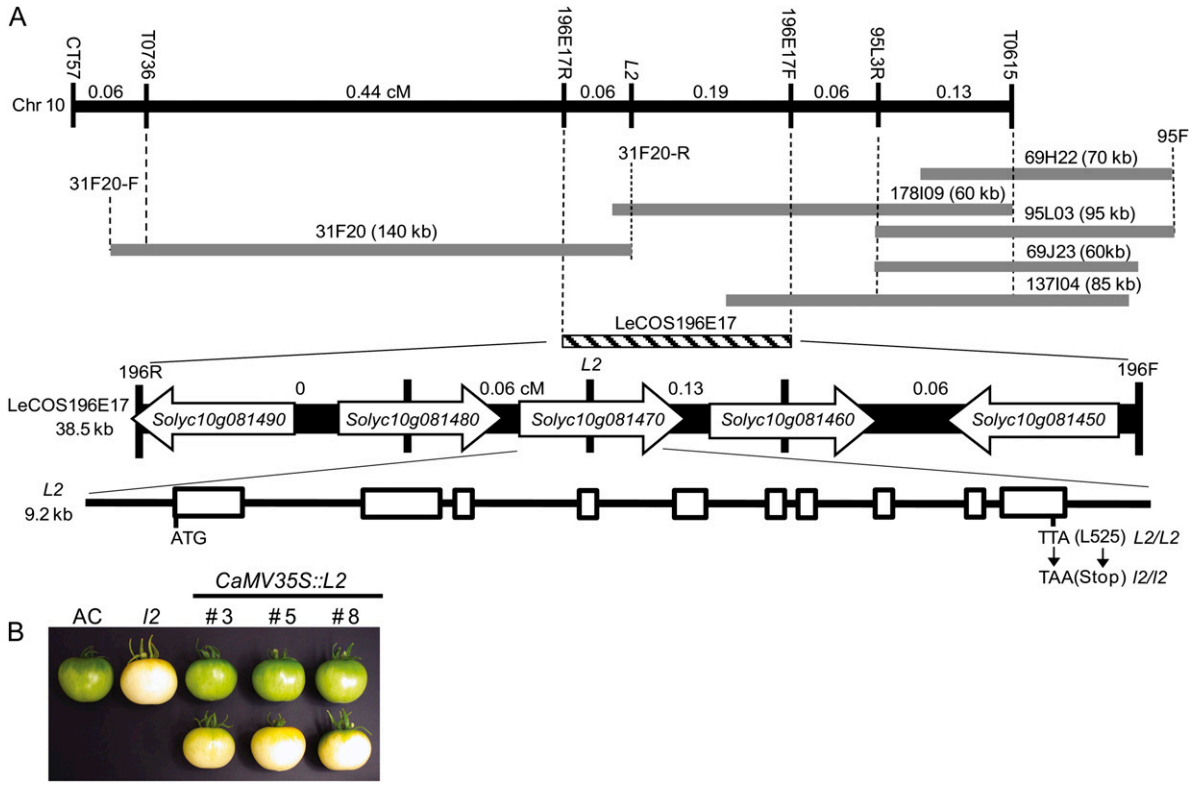


**Figure 5.** Positional cloning of the *L2* locus. A, Genetic and physical map of the *l2* locus derived using an interspecific F2 population of 799 plants. Distances between adjacent RFLP markers are given in cM. BAC clones isolated using the RFLP markers T0615 and T0736 are shown as gray bars. BAC ends were isolated as described in the text and given F and R designations. A cosmid clone, LeCOS196E17, isolated using 31F20-R is represented as a striped bar. Vertical dashed lines are shown to indicate relative positions of genetic markers and genomic clones. LeCOS196E17 contains five predicted genes (*Solyc10g081450–Solyc10g081490*). The genetic distance between these genes is shown in cM. *Solyc10g081470* cosegregates with the *l2* phenotype and has a structure comprised of 10 exons separated by nine introns. The T → A substitution in exon 10 that converts Leu 525 to a stop codon in *l2* is shown. B, Complementation of the *l2* mutant phenotype. Mature green fruit from three independently transformed segregating T1 lines containing the transgene (top section) and without the transgene (bottom section). AC and *l2* fruits are shown for phenotypic comparison.

*Solyc10g081470* cDNA was expressed under the control of the cauliflower mosaic virus *35S* promoter in the *l2* mutant background. Nineteen out of 22 independently transformed primary transformants recovered showed complementation of the *l2* phenotype, determined by chlorophyll content of mature green fruit. Three lines were selected for subsequent analysis in the T1 generation (Fig. 5B). Typical phenotypes of AC and *l2* mature green fruits are shown along with three independent T1 lines segregating for the *NPTII* selectable marker. Fruits from plants in the top section contained *NPTII* and showed complementation of the *l2* mutant phenotype. Conversely the fruit on the bottom section came from plants that had segregated out the *NPTII* gene and had reverted to the *l2* mutant phenotype.

### *L2* Encodes a Tomato Homolog of Arabidopsis *EGY1*

*L2* (*Solyc10g081470*) encodes a predicted protein of 547 amino acids with a molecular mass of 58.4 kD. A BlastP search using the predicted L2 protein as the query sequence revealed homology to proteins from several higher plant species and other photosynthetic organisms, including bryophytes, algae, and cyanobacteria. Significantly, the Arabidopsis protein displaying the highest similarity to L2 (73% identical/82% similarity) was encoded by the *EGY1* locus, a chloroplast-targeted member of the zinc-dependent M50 family of metalloproteases (http://merops.sanger.ac.uk) that is required for normal plastid development and gravitropic response in Arabidopsis (Chen et al., 2005). The M50 family is diverse, with members from bacteria, archaea, protozoa, plants animals, and some fungi. The family is characterized by two conserved domains, HEXXH and NXXPXXXLDG that are present in L2 and related homologs (Fig. 6). These two domains are predicted to form the active site with Glu acting as the catalytic residue and the histidines and Asp residues coordinating the zinc ions. Mutant studies have demonstrated the importance of these domains for catalytic activity (Rawson et al., 1997; Rudner et al., 1999). A second feature of this

family is that they are integral membrane proteins with the active site domains lying within, or in close proximity to, the membrane-spanning domains (Fig. 6). The Aramemnon Plant Membrane Database (http://aramemnon.botanik.uni-koeln.de/index.ep), which collates the membrane topology predictions of several algorithms, predicts that Arabidopsis EGY1 contains eight transmembrane-spanning domains (Fig. 6). A search utilizing the TMHMM server version 2.0 (http://www.cbs.dtu.dk) revealed that the predicted L2 protein has six transmembrane-spanning domains with an additional two domains lying slightly below

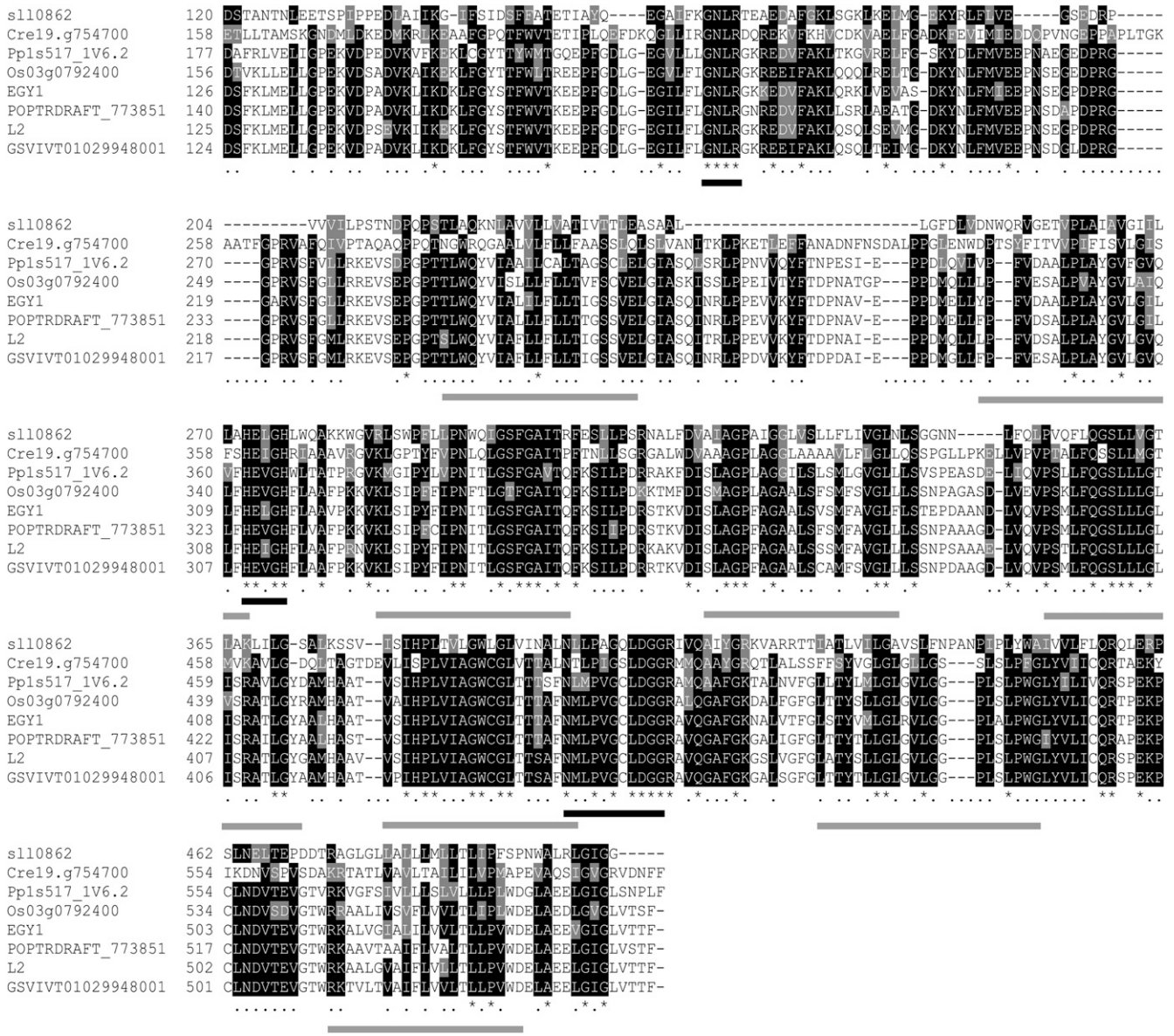


**Figure 6.** Amino acid alignment of L2-related proteins. Alignments based on the conserved region of L2 related proteins were generated using MUSCLE. Conserved amino acids are indicated by shaded squares. The highly conserved motifs characteristic of these proteins, GNLR, HEXXH, and NXXPXXLDG are underlined with solid black lines. The solid gray lines depict the predicted transmembrane helices for EGY1 as determined by the TmConsens algorithm (http://aramemnon.botanik.uni-koeln.de/index.ep). Accession numbers of the sequences are as follows: L2 (JQ683149), *Vitis vinifera* GSVIVT01029948001 (XP_002269447), *Populus trichocarpa* POPTRDRAFT_773851 (XP_002319720), rice Os03g0792400 (EEE60079), *Synechocystis* sp. PCC 6803 sll0862 (NP_440944). The sequence of Arabidopsis EGY1 is based on annotation available at The Arabidopsis Information Resource (http://www.arabidopsis.org) and the sequences of Cre19.g754700 and Ppls517_1V6.2 are based on annotations of the *C. reinhardtii* and *Physcomitrella patens* genomes available through the Phytozome database (http://www.phytozome.net/).

the threshold of probability. Similarly, the selection of EGY1/L2 homologs depicted in Figure 6 are all predicted to contain between six and eight transmembrane-spanning domains lying in relatively conserved positions (data not shown). Localization experiments utilizing an Arabidopsis EGY1-GFP fusion demonstrated that EGY1 is targeted to the chloroplast (Chen et al., 2005). Similarly, in silico prediction of L2 subcellular localization using the Predotar server (http://urgi.versailles.inra.fr/predotar/predotar.html) resulted in a probability estimate of 0.79 for plastid localization.

### Identification of Additional Alleles at the *l2* Locus

A second putative *l2* allele was reported as a spontaneous mutation in a trial plot of the cultivar Fireball in 1960 and was designated Lutescent Fireball (Kerr et al., 1975; Supplemental Fig. S3). An allelism test confirmed that F1 progeny of a cross between Lutescent Fireball and the original *l2* allele in the Long Red variety displayed a typical lutescent phenotype (Kerr et al., 1975). RT-PCR amplification of *L2* from cv Fireball yielded the expected transcript of 1,641 bp that was identical to that obtained from cv AC. In contrast, amplification of the *L2* cDNA from Lutescent Fireball revealed multiple products of a slightly altered size (Fig. 7A). Sequence analysis of these RT-PCR products revealed the existence of four distinct *L2* transcripts in the Lutescent Fireball cultivar ranging in size between 1,572 and 1,846 bp, each with aberrant splicing occurring between intron 7 and exon 8. Three of the splice variants (SV2, SV3, and SV4) cause frame-shift mutations, leading to incorporation of several spurious amino acids followed by premature stop codons that truncate the predicted L2 protein between 79 and 85 amino acids (Fig. 7B). In contrast the SV1 splice variant causes an in-frame deletion of the entire eighth exon, leading to the removal of 23 amino acids between Q455 and L479 (Fig. 7C). Furthermore, the wild-type transcript was not detected in the Lutescent Fireball cultivar, suggesting that the L2 protein may be nonfunctional in this variety. To further explore the possibility that a splicing defect in *L2* is the underlying cause of the Lutescent Fireball phenotype, a 750-bp genomic fragment spanning exons 7 and 8 from in both Fireball and Lutescent Fireball revealed a G → A nucleotide change at position 7000 of the *L2* genomic clone in the Lutescent Fireball cultivar (Fig. 7B). This single nucleotide substitution disrupts the consensus splice acceptor site at the boundary between intron 7 and exon 8 (CAG → CAA). Together, these data suggest that the phenotype of Lutescent Fireball is caused by aberrant splicing, resulting in the failure to produce a mature *L2* transcript. A third mutant resembling *l2*, e3779 that figures prominently in the characterization described here, was recovered from an EMS mutagenized population of the M82 cultivar (Menda et al., 2004; Supplemental Fig. S2). Sequence analysis of the *L2* cDNA amplified from e3779 revealed the deletion of a G nucleotide at position 1575 that results in a frame-shift mutation that

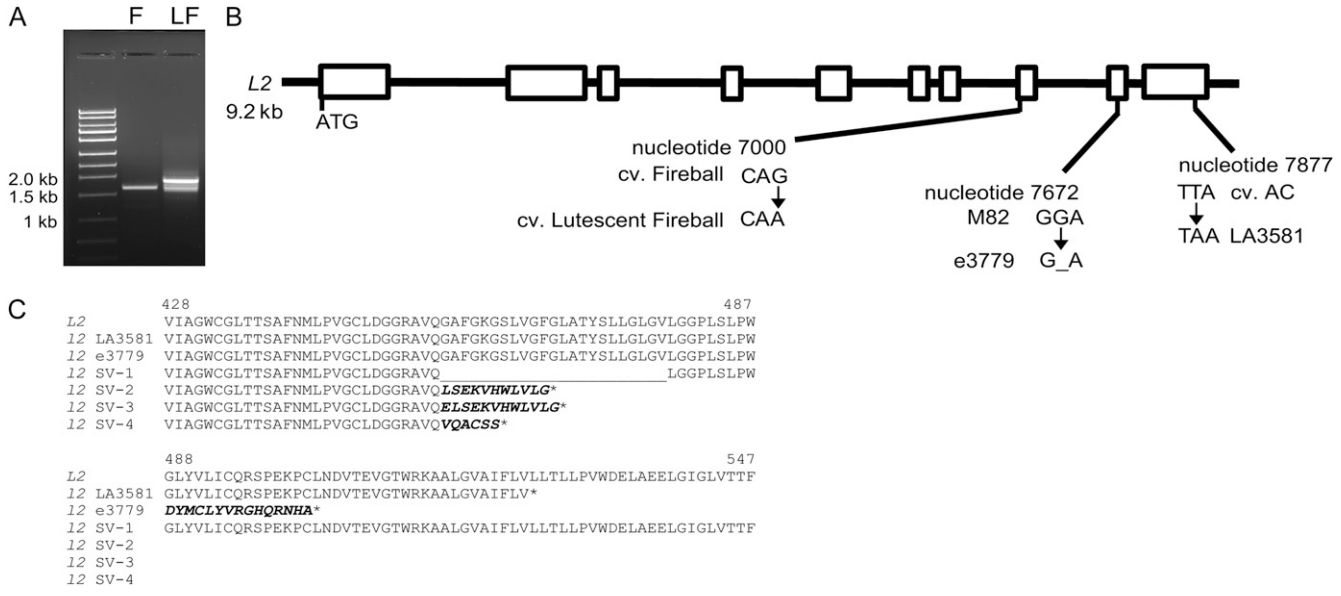


**Figure 7.** Identification of additional *l2* mutant alleles. A, Aberrant splicing of *L2* in the Lutescent Fireball cultivar. RT-PCR amplification of cDNA fragments corresponding to *L2* from Fireball (F) and Lutescent Fireball (LF) cultivars. The approximate size of the DNA fragments is indicated. B, Relative positions and nucleotide changes observed in the *l2* mutant alleles identified in the Lutescent Fireball cultivar and in the EMS derived mutant e3779. White boxes correspond to exons. C, Consequences of *l2* mutant alleles on the predicted L2 protein sequence.

removes Gly 488, resulting in the incorporation of 15 spurious amino acids before terminating in a premature stop codon (Fig. 7, B and C).

## DISCUSSION

### The Role of L2 in Chloroplast Function

The nonallelic *l1* and *l2* mutants display pleiotropic phenotypes that are consistent with defects in chloroplast development (Figs. 1 and 2). These data are supported by the finding that *L2* encodes an ortholog of Arabidopsis *EGY1*, mutations that disrupt plastid number and development, leading to impaired formation of the thylakoid membranes and reduced accumulation of chlorophyll *a*/*b*-binding proteins of the light-harvesting complexes I and II (Chen et al., 2005; Guo et al., 2008). However, a notable difference between *l2* and *egy1* mutant alleles is that while *egy1* mutant alleles have reduced chlorophyll content and are pale throughout development (Chen et al., 2005), leaves of *l2* mutants are slow to deetiolate (Fig. 2) but eventually accumulate close to wild-type levels of chlorophyll prior to undergoing premature chlorophyll loss later in development (Fig. 2C). Furthermore, altered patterns of chlorophyll accumulation are evident between leaf and reproductive tissues of *lutescent* mutants. For example, while *l1* and *l2* leaves accumulate chlorophyll, the pistils and fruits of the mutants display greatly impaired chlorophyll accumulation from early in development and therefore resemble the pale phenotype of *egy1* mutant alleles (Fig. 1). The basis for these differences, particularly the seemingly less significant role that L2 plays in chlorophyll accumulation in tomato leaves, is currently not understood.

In addition to a role in mediating chlorophyll accumulation during development, evidence suggests that *EGY1/L2* and related homologs may play a role in mediating chloroplast responses to environmental conditions. For example, both *l1* and *l2* mutants are hypersensitive to darkness and high-light stress, leading to enhanced chlorosis (Fig. 1, G and H) and EGY1 protein levels in Arabidopsis are influenced by dark/light cycles with increased abundance evident in light-grown tissues (Chen et al., 2005). Similarly, iron deficiency, a stress known to reduce photosynthetic electron transfer, resulted in increased accumulation of the EGY1/L2 homolog, C_770040, from *Chlamydomonas reinhardtii* (Naumann et al., 2007). Furthermore, publically available Arabidopsis gene expression data revealed that *EGY1* is induced under both high-light treatments and iron deficiency together with other biotic and abiotic stresses (Zimmermann et al., 2004). Together these data suggest a role for EGY1/L2 in both the early steps of chloroplast development and the maintenance of chloroplast homeostasis in response to environmental perturbation.

EGY1 and L2 belong to the M50 family of metalloproteases and each contains motifs known to be required for the activity of functionally characterized members of this family (Fig. 6). While considerable progress has been made on elucidating the role of chloroplast-localized proteases (Kato and Sakamoto, 2010), the exact biochemical function of EGY1/L2 and other plant M50 proteases, including the identity of their in vivo substrates remains unknown. Members of the M50 family of proteases are integral membrane proteins with their active sites residing within or adjacent to the membrane (Fig. 6). The M50 family belong to a category of proteases referred to as intramembrane cleaving proteases that are involved in the regulation of cellular responses to metabolic status and stress that participate in a general phenomenon known as regulated intramembrane proteolysis (RIP). For example, the founder member of the M50 family, the sterol-regulatory element binding protein (SREBP) site-2 protease regulates sterol biosynthesis and uptake in mammalian cells through release of the membrane-bound transcription factor SREBP in a pathway that involves trafficking of the sequestered SREBP from the endoplasmic reticulum to the Golgi under low-sterol conditions (Osborne and Espenshade, 2009). Similar two-step proteolysis occurs in response to stress in bacteria, allowing the release of membrane-bound transcription factors (Rudner et al., 1999; Alba et al., 2002; Kanehara et al., 2002). Far less is known about RIP in plants. Membrane-tethered transcription factors have been identified in plants and in a few instances proteolytic cleavage of these transcription factors has been demonstrated but none of these have been reported to involve transcription factors that are sequestered in the chloroplast (Seo et al., 2008; Kim et al., 2010; Liu and Howell, 2010). Therefore, it is possible that EGY1/L2 proteases participate in chloroplast-localized phenomena such as processing or degradation of proteins at the thylakoid membrane during photosystem assembly or in response to environmental perturbation and disruption of photosynthetic function. Examples of proteolysis and processing in the chloroplast are already well characterized and are involved in the turnover and repair of photosystem proteins in response to photoinhibition and abiotic stress (Kato and Sakamoto, 2010; Sun et al., 2010).

### *lutescent* Mutants and Their Impact on Fruit Development and Ripening

Both *l1* and *l2* mutants exhibited a delay in the onset of fruit ripening (Fig. 4). However, once ripening is initiated in *l1* and *l2* fruits the rate of ripening appears normal and mutant fruits accumulate wild-type levels and composition of carotenoids (Supplemental Fig. S1), suggesting that a fully functional chloroplast is not required for chromoplast development in tomato. The concept of separation of chloroplast and chromoplast development is also observed in stay-green mutants of tomato and pepper that undergo typical chromoplast development in the absence of chlorophyll breakdown

and thylakoid membrane dissolution (Cheung et al., 1993; Roca et al., 2006).

As *l1* and *l2* mutants have disrupted chloroplast function, it is likely that the delayed fruit ripening phenotypes observed in mutant fruit arise as an indirect consequence of an altered chloroplast-derived signal that promotes the onset of ripening. The recent finding that disruption of Glu-1-semialdehyde aminotransferase activity in tomato fruits alters early seed development (Lytovchenko et al., 2011) provides a possible mechanism that could ultimately lead to a delay in the onset of ripening. It will be of interest to examine the rates of ripening in Glu-1-semialdehyde aminotransferase-silenced lines and early seed development in *l1* and *l2* mutants, particularly as fruit of *lutescent* mutants are also compromised in their photosynthetic capacity (Fig. 3A).

Alternatively, lower chloroplast numbers in developing fruits of *l1* and *l2* could be supportive of reduced levels of a factor that promotes ripening. The nature of the signals that stimulate ripening are not fully understood, although multiple factors including ethylene are known to play a role in ripening induction (Srivastava and Handa, 2005; Barry and Giovannoni, 2007; Zhang et al., 2009; Barry, 2010). The ability of ethylene to trigger rapid and normal ripening of *l1* and *l2* fruit at the mature green stage of development, coupled with the delay in the onset of ethylene synthesis suggests that *l1* and *l2* fruit possess a typical response to ethylene but may be perturbed in the ability to initiate the ripening-related increase in ethylene production (Fig. 4; Supplemental Fig. S1). Recent characterization of the $Orr^{DS}$ mutant of tomato that encodes the M subunit of the chloroplast-localized NADH dehydrogenase complex, also supports a role for a chloroplast-derived signal that promotes ripening (Nashilevitz et al., 2010). The $Orr^{DS}$mutant exhibits a delay in the onset of fruit ripening and ripening-related ethylene biosynthesis. Although the reason for this delay is not fully understood, the $Orr^{DS}$ mutant has a 30% to 40% reduction in the levels of both Ser and Asp, two chloroplast-derived amino acids that are precursors of Met, which serves as the precursor of ethylene (Nashilevitz et al., 2010). It will be of interest to determine whether chloroplast metabolism in *l1* and *l2* fruit influences seed development and precursor pools for the synthesis of hormones and to define whether a link exists between these factors and the observed delay in the onset of fruit ripening.

## CONCLUSION

Cloning of the *L2* gene has identified a link between chloroplast development and as-yet-unidentified factors that influence the onset of fruit ripening. The mechanism of this interaction, together with the specific biochemical activity of EGY1/L2 and the potential role of these proteins in RIP remain to be identified. In this regard, we have shown that the *l1* mutant, which resides at a distinct locus on chromosome 8 (Tanksley et al., 1992), possesses an identical phenotype to that of *l2*, suggesting the strong possibility that the underlying gene may be functionally related to *L2*. Therefore, identification of the gene underlying the *l1* mutant phenotype may provide insight into the molecular function of EGY1/L2 in plants.

## MATERIALS AND METHODS

### Plant Material and Treatments

Tomato (*Solanum lycopersicum*) seeds homozygous for the *l1* (LA3717) and *l2* (LA3581) mutations and *Solanum galapagense* (LA0483) were obtained from the Tomato Genetics Resource Center, University of California, Davis. The parental cultivar AC was originally obtained from the Glasshouse Crops Research Institute (Littlehampton, Sussex, UK). Seeds of the cultivars Fireball (CN 18026) and Lutescent Fireball (CN 1586) were obtained from Plant Gene Resources of Canada. Seeds of the EMS mutant, e3779 and the M82 parental cultivar were provided by Dani Zamir (Hebrew University of Jerusalem). Tomato plants were grown in peat-based compost supplemented with fertilizer in greenhouses equipped with heating and cooling systems and supplemental lighting either at Cornell University, Ithaca, New York or at Michigan State University, East Lansing, Michigan and under greenhouse conditions at Hebrew University of Jerusalem, Israel or in the field at an experimental station in Akko, Israel.

Evaluation of the deetiolation response of tomato seedlings was performed as follows. Surface-sterilized seeds were sown on 1% water agar supplemented with 0.5× Murashige and Skoog salts pH 5.6 and incubated in the dark for 7 d at 25°C. The germinated seedlings were then exposed to light for up to 24 h and the cotyledons excised and either immediately frozen in liquid $N_2$ or immersed in fixative for transmission electron microscopy (described below). Experiments to evaluate the triple-response phenotype in dark-grown tomato seedlings were performed as previously described (Barry et al., 2005) with the exception that seedlings were measured at 8 d after sowing. Ethylene treatments were performed by sealing fruits at the mature green stage of development in glass canning jars of a known volume and exposing to 10 $\mu$L $L^{-1}$ of ethylene for 24 h. Following ethylene treatments fruits were held at room temperature for 72 h and ripening evaluated. For evaluation of response to high-light conditions plants were grown under a 16 h photoperiod at 27°C/20°C day/night temperature and a light intensity of 500 $\mu$mol $m^{-2}$ $s^{-1}$. Plants were photographed 3 weeks after germination.

### Ethylene Measurements

Mature green fruit were harvested and held at room temperature for 24 h. For ethylene determination, fruits were sealed each day for 2 h in glass jars and a 1-mL headspace sample was analyzed by gas chromatography using a Carle AGC series 100 gas chromatograph equipped with an activated alumina column and flame ionization detector, as previously described (Watkins et al., 2004).

### Measurements of Photosynthetic Efficiency

The efficiency of PSII was estimated by measuring chlorophyll fluorescence with a computer-controlled pulse amplitude modulated fluorometer IMAG-MAX/L (Walz). Detached fruit were dark adapted for 20 min. A 2-cm-thick slice was cut and placed in the measuring chamber with the fruit surface facing up toward the measuring beam. A low (0.1 $\mu$mol photons $m^{-2}$ $s^{-1}$) modulated (1.6 kHz) measuring light was used to determine the minimal fluorescence level, followed by a 1 s of saturating white light pulse of 1,500 $\mu$mol photons $m^{-2}$ $s^{-1}$ to obtain the maximal fluorescence level. The fruit was then illuminated with continuous actinic red light (650 nm, 40-$\mu$mol photons $m^{-2}$ $s^{-1}$), until a steady-state fluorescence was reached (up to 10 min). A second saturating pulse was then applied to determine the maximal fluorescence level in the light-adapted state.

### Pigment Analysis

Chlorophyll was extracted from tissues in acetone and quantified as previously described (Lichtenthaler, 1987). Fruit carotenoids were analyzed by HPLC as previously described (Ronen et al., 1999).

## Confocal Laser-Scanning Microscopy

The chloroplasts of tomato fruit were imaged using an Olympus FluoView FV1000 laser-scanning confocal microscope. Chlorophyll autofluorescence was detected with a 650 to 750 nm band pass filter following excitation at 488 nm with an argon laser line. Cells were visualized using differential interference contrast transmitted light microscopy using a 20× UPlan SApo objective with a numerical aperture of 0.75. Images were merged using Olympus FluoView software.

## Transmission Electron Microscopy

Cotyledons were fixed in a mixture of 2.5% glutaraldehyde and 2.5% paraformaldehyde in 0.1 M cacodylate buffer at 4°C for 24 h, postfixed in 1% osmium tetroxide, and dehydrated in a graded acetone series. Samples were infiltrated and embedded in Poly/Bed 812 resin (Polysciences Inc.). Thin sections (70-nm thickness) were obtained with a PTXL ultramicrotome (RMC, Boeckeler Instruments) on 200 mesh copper grids stained with uranyl acetate and lead citrate. Sections were imaged using a JEOL 100CX transmission electron microscope (JEOL) at a 100-kV accelerating voltage.

## Genetic and Physical Mapping of the *l2* Locus

An interspecific F2 mapping population was generated from the following cross tomato (*l2*/*l2*) (LA3581) × *S. galapagense* (*L2*/*L2*; LA0483). Genomic DNA isolation and molecular mapping using RFLP markers was performed as previously described (Barry et al., 2005). Details of tomato genetic maps and the chromosome 10 molecular markers can be accessed through the Solanaceous Genomics Network (http://solgenomics.net/). Restriction enzymes yielding RFLPs between tomato and *S. galapagense* for given DNA probes are as follows; T736: *Hae*III, CT57: *Nde*I, T615: *Nla*IV, 95R: *Ava*II, 196E17F: *Xba*I, 196E17R: *Eco*RV, cLET10H23: *Rsa*I, *L2*: *Apo*I, cTOF24I6: *Nsi*I. A physical contig spanning the *L2* locus was obtained via screening and characterization of ordered bacterial artificial chromosome (BAC) and cosmid libraries derived from tomato, *Solanum pennellii*, and *S. galapagense* (Li et al., 2005; Chen et al., 2007). Clones LA0483BAC69H22, LA0483BAC69J23, and LA0483BAC178I9 were isolated from an *S. galapagense* library. Clones LpenCOS31F20, LpenCOS95L3, and LpenBAC137I4 were isolated from two *S. pennellii* libraries. The approximate size of each BAC clone was determined by pulsed-field gel electrophoresis. BAC and cosmid ends were isolated by direct DNA sequencing and converted to RFLP markers for further genetic and physical mapping. Subcloning of the tomato cosmid clone LeCOS196E17 was achieved by three separate restriction enzyme digests (*Bam*HI, *Eco*RI, and *Hin*DIII) followed by ligation into pBluescript SK− (Stratagene), previously linearized with the same restriction enzymes. The resultant clones were sequenced with vector primers to yield a number of anchor points that were subsequently utilized to extend and complete the sequence of LeCOS196E17 using multiple rounds of primer extension.

## RNA Isolation and Cloning of *L2* cDNA and Genomic Fragments

RNA was extracted from leaf and fruit tissues using either previously described methods or the RNeasy plant mini kit (Qiagen; Griffiths et al., 1999; Barry et al., 2005). cDNA synthesis was performed using the transcriptor first-strand cDNA synthesis kit (Roche Applied Science). The coding region of *L2* was amplified by RT-PCR using cDNA synthesized from RNA extracted from leaf of either wild-type (*L2*/*L2*) or mutant (*l2*/*l2*) genotypes using the primers L2PROT-F: 5′-GGACTTTTATCAAACAGCTAACTTGCA-3′ and L2PROT-R: 5′-GGCACAACCCAACTTACAATAATTGTA-3′. Detection of the point mutation in the $l2^{Fireball}$ allele was achieved through amplification of a genomic fragment spanning exons 7 and 8 from the Fireball and Lutescent Fireball cultivars using the primers L2GEN-1F: 5′-GGTAATTTTCAGCATGCTTGGTCTA-3′ and L2GEN-1R: 5′-GAGAATCACAGGCATTTGATCTAC-3′. Fragments were amplified using the *Pfu* Ultra DNA polymerase (Agilent Technologies) and cloned into either *Eco*RV linearized pBluescript SK− (Agilent Technologies) using standard cloning techniques or into pCR4Blunt-TOPO vector (Invitrogen Corporation). Sequencing of inserts was accomplished using vector primers and the gene-specific primers L2PROT-1: 5′-GAGCTAGGAATTGCGTCTCA-3′, L2PROT-2: 5′-TGAGACGCAATTCCTAGCTC-3′, L2PROT-3: 5′-TGCTACCAGTTGGATGTCTT-3′, and L2PROT-4: 5′-AAGACATCCAACTGGTAGCA-3′.

## DNA Constructs and Plant Transformation

The *L2* cDNA insert was released from pBluescript SK− by digestion with *Xba*I and *Sac*I. The fragment was ligated downstream of the cauliflower mosaic virus *35S* promoter in the binary vector pBI121, previously modified by removal of the *UidA* coding region by digestion with the same restriction enzymes. Transgenic tomato plants were generated through cotyledon-derived explants via *Agrobacterium tumefaciens* mediated transformation (strain LBA4404), using previously described methods (Fillatti et al., 1987). Transgene integration was determined by a combination of gel-blot and PCR analysis.

## DNA Sequence Analysis and Bioinformatics Resources

DNA sequences were assembled using Sequencher version 4.7 (Genecodes Corporation). The prediction of genes within genomic DNA sequence was performed using the FGENESH hidden Markov model-based gene structure prediction program (http://linux1.softberry.com/berry.phtml). Amino acid alignments were generated using MUSCLE (Edgar, 2004) and were decorated using the Boxshade server version 3.2.1 (http://www.ch.embnet.org). Analysis of membrane-spanning domains was accomplished using the Aramemnon database (http://aramemnon.uni-koeln.de/; Schwacke et al., 2003) and prediction of chloroplast transit peptides was accomplished using the Predotar prediction server (http://urgi.versailles.inra.fr/predotar/predotar.html).

## Statistical Analysis

Statistical analyses were performed using SAS (SAS Institute, www.sas.com). The genotypic constituents were evaluated using least squares means.

Sequences reported in this manuscript have been deposited in GenBank under the following accession number: JQ683149.

## Supplemental Data

The following materials are available in the online version of this article.

**Supplemental Figure S1.** Carotenoid composition in ripe fruits of the *lutescent* mutants.

**Supplemental Figure S2.** The *lutescent* mutants have a normal ethylene response.

**Supplemental Figure S3.** Phenotypes of additional *l2* alleles.

## ACKNOWLEDGMENTS

We thank Drs. Alicia Pastor and Melinda Frame (Center for Advanced Microscopy, Michigan State University) for assistance with transmission electron microscopy and confocal laser-scanning microscopy, respectively.

Received March 19, 2012; accepted May 21, 2012; published May 22, 2012.

## LITERATURE CITED

**Ajjawi I, Lu Y, Savage LJ, Bell SM, Last RL** (2010) Large-scale reverse genetics in Arabidopsis: case studies from the Chloroplast 2010 Project. Plant Physiol **152:** 529–540

**Alba BM, Leeds JA, Onufryk C, Lu CZ, Gross CA** (2002) DegS and YaeL participate sequentially in the cleavage of RseA to activate the sigma(E)-dependent extracytoplasmic stress response. Genes Dev **16:** 2156–2168

**Armbruster U, Pesaresi P, Pribil M, Hertle A, Leister D** (2011) Update on chloroplast research: new tools, new topics, and new trends. Mol Plant **4:** 1–16

**Barry CS** (2010) Factors influencing the ripening and quality of fleshy fruits. *In* L Ostergaard, ed, Annual Plant Reviews, Vol 38. Wiley-Blackwell, Oxford, UK, pp 296–326

**Barry CS, Giovannoni JJ** (2007) Ethylene and fruit ripening. J Plant Growth Regul **26:** 143–159

**Barry CS, McQuinn RP, Chung M-Y, Besuden A, Giovannoni JJ** (2008) Amino acid substitutions in homologs of the STAY-GREEN protein are

responsible for the *green-flesh* and *chlorophyll retainer* mutations of tomato and pepper. Plant Physiol **147:** 179–187

**Barry CS, McQuinn RP, Thompson AJ, Seymour GB, Grierson D, Giovannoni JJ** (2005) Ethylene insensitivity conferred by the *Green-ripe* and *Never-ripe 2* ripening mutants of tomato. Plant Physiol **138:** 267–275

**Bino RJ, Ric de Vos CH, Lieberman M, Hall RD, Bovy A, Jonker HH, Tikunov Y, Lommen A, Moco S, Levin I** (2005) The light-hyperresponsive high pigment-2dg mutation of tomato: alterations in the fruit metabolome. New Phytol **166:** 427–438

**Borovsky Y, Paran I** (2008) Chlorophyll breakdown during pepper fruit ripening in the *chlorophyll retainer* mutation is impaired at the homolog of the senescence-inducible stay-green gene. Theor Appl Genet **117:** 235–240

**Chai YM, Jia HF, Li CL, Dong QH, Shen YY** (2011) *FaPYR1* is involved in strawberry fruit ripening. J Exp Bot **62:** 5079–5089

**Chen G, Bi YR, Li N** (2005) *EGY1* encodes a membrane-associated and ATP-independent metalloprotease that is required for chloroplast development. Plant J **41:** 364–375

**Chen GP, Hackett R, Walker D, Taylor A, Lin ZF, Grierson D** (2004) Identification of a specific isoform of tomato lipoxygenase (*TomloxC*) involved in the generation of fatty acid-derived flavor compounds. Plant Physiol **136:** 2641–2651

**Chen KY, Cong B, Wing R, Vrebalov J, Tanksley SD** (2007) Changes in regulation of a transcription factor lead to autogamy in cultivated tomatoes. Science **318:** 643–645

**Cheung A-Y, McNellis T, Piekos B** (1993) Maintenance of chloroplast components during chromoplast differentiation in the tomato mutant *green flesh*. Plant Physiol **101:** 1223–1229

**Chung MY, Vrebalov J, Alba R, Lee J, McQuinn R, Chung JD, Klein P, Giovannoni J** (2010) A tomato (*Solanum lycopersicum*) *APETALA2/ERF* gene, *SlAP2*a, is a negative regulator of fruit ripening. Plant J **64:** 936–947

**Edgar RC** (2004) MUSCLE: multiple sequence alignment with high accuracy and high throughput. Nucleic Acids Res **32:** 1792–1797

**Fankhauser C, Chory J** (1997) Light control of plant development. Annu Rev Cell Dev Biol **13:** 203–229

**Fillatti JJ, Kiser J, Rose R, Comai L** (1987) Efficient transfer of a glyphosate tolerance gene into tomato using a binary *Agrobacterium-tumefaciens* vector. Bio-Technology **5:** 726–730

**Galpaz N, Wang Q, Menda N, Zamir D, Hirschberg J** (2008) Abscisic acid deficiency in the tomato mutant *high-pigment 3* leading to increased plastid number and higher fruit lycopene content. Plant J **53:** 717–730

**Griffiths A, Barry C, Alpuche-Solis A-G, Grierson D** (1999) Ethylene and developmental signals regulate expression of lipoxygenase genes during tomato fruit ripening. J Exp Bot **50:** 793–798

**Guo D, Gao XR, Li H, Zhang T, Chen G, Huang PB, An LJ, Li N** (2008) EGY1 plays a role in regulation of endodermal plastid size and number that are involved in ethylene-dependent gravitropism of light-grown Arabidopsis hypocotyls. Plant Mol Biol **66:** 345–360

**Herner RC, Sink KC** (1973) Ethylene production and respiratory behavior of the *rin* tomato mutant. Plant Physiol **52:** 38–42

**Itkin M, Seybold H, Breitel D, Rogachev I, Meir S, Aharoni A** (2009) *TOMATO AGAMOUS-LIKE 1* is a component of the fruit ripening regulatory network. Plant J **60:** 1081–1095

**Jaakola L, Poole M, Jones MO, Kämäräinen-Karppinen T, Koskimäki JJ, Hohtola A, Häggman H, Fraser PD, Manning K, King GJ, et al** (2010) A *SQUAMOSA MADS* box gene involved in the regulation of anthocyanin accumulation in bilberry fruits. Plant Physiol **153:** 1619–1629

**Jia HF, Chai YM, Li CL, Lu D, Luo JJ, Qin L, Shen YY** (2011) Abscisic acid plays an important role in the regulation of strawberry fruit ripening. Plant Physiol **157:** 188–199

**Kanehara K, Ito K, Akiyama Y** (2002) YaeL (EcfE) activates the sigma(E) pathway of stress response through a site-2 cleavage of anti-sigma(E), RseA. Genes Dev **16:** 2147–2155

**Karlova R, Rosin FM, Busscher-Lange J, Parapunova V, Do PT, Fernie AR, Fraser PD, Baxter C, Angenent GC, de Maagd RA** (2011) Transcriptome and metabolite profiling show that *APETALA2a* is a major regulator of tomato fruit ripening. Plant Cell **23:** 923–941

**Kato Y, Sakamoto W** (2010) New insights into the types and function of proteases in plastids. Int Rev Cell Mol Biol **280:** 185–218

**Kerr EA** (1956) lutescent 2, l2. Report of the Tomato Genetics Cooperative **6:** 17

**Kerr EA, Lyall LH, Graham TO** (1975) A mutation to *lutescent-2* in "Fireball". Report of the Tomato Genetics Cooperative **25:** 10

**Kim SG, Lee S, Seo PJ, Kim SK, Kim JK, Park CM** (2010) Genome-scale screening and molecular characterization of membrane-bound transcription factors in Arabidopsis and rice. Genomics **95:** 56–65

**Klee HJ** (2010) Improving the flavor of fresh fruits: genomics, biochemistry, and biotechnology. New Phytol **187:** 44–56

**Klee HJ, Giovannoni JJ** (2011) Genetics and control of tomato fruit ripening and quality attributes. Annu Rev Genet **45:** 41–59

**Kolotilin I, Koltai H, Tadmor Y, Bar-Or C, Reuveni M, Meir A, Nahon S, Shlomo H, Chen L, Levin I** (2007) Transcriptional profiling of high pigment-2dg tomato mutant links early fruit plastid biogenesis with its overproduction of phytonutrients. Plant Physiol **145:** 389–401

**Kovács K, Fray RG, Tikunov Y, Graham N, Bradley G, Seymour GB, Bovy AG, Grierson D** (2009) Effect of tomato pleiotropic ripening mutations on flavour volatile biosynthesis. Phytochemistry **70:** 1003–1008

**Lee JM, Joung J-G, McQuinn R, Chung M-Y, Fei Z, Tieman D, Klee H, Giovannoni J** (2012) Combined transcriptome, genetic diversity and metabolite profiling in tomato fruit reveals that the ethylene response factor *SlERF6* plays an important role in ripening and carotenoid accumulation. Plant J **70:** 191–204

**Li CY, Schilmiller AL, Liu GH, Lee GI, Jayanty S, Sageman C, Vrebalov J, Giovannoni JJ, Yagi K, Kobayashi Y, et al** (2005) Role of beta-oxidation in jasmonate biosynthesis and systemic wound signaling in tomato. Plant Cell **17:** 971–986

**Lichtenthaler HK** (1987) Chlorophylls and carotenoids—pigments of photosynthetic biomembranes. Methods Enzymol **148:** 350–382

**Lisso J, Altmann T, Müssig C** (2006) Metabolic changes in fruits of the tomato dx mutant. Phytochemistry **67:** 2232–2238

**Liu JX, Howell SH** (2010) Endoplasmic reticulum protein quality control and its relationship to environmental stress responses in plants. Plant Cell **22:** 2930–2942

**Lytovchenko A, Eickmeier I, Pons C, Osorio S, Szecowka M, Lehmberg K, Arrivault S, Tohge T, Pineda B, Anton MT, et al** (2011) Tomato fruit photosynthesis is seemingly unimportant in primary metabolism and ripening but plays a considerable role in seed development. Plant Physiol **157:** 1650–1663

**Manning K, Tör M, Poole M, Hong Y, Thompson AJ, King GJ, Giovannoni JJ, Seymour GB** (2006) A naturally occurring epigenetic mutation in a gene encoding an SBP-box transcription factor inhibits tomato fruit ripening. Nat Genet **38:** 948–952

**Martel C, Vrebalov J, Tafelmeyer P, Giovannoni JJ** (2011) The tomato MADS-box transcription factor RIPENING INHIBITOR interacts with promoters involved in numerous ripening processes in a *COLORLESS NONRIPENING*-dependent manner. Plant Physiol **157:** 1568–1579

**Menda N, Semel Y, Peled D, Eshed Y, Zamir D** (2004) *In silico* screening of a saturated mutation library of tomato. Plant J **38:** 861–872

**Nakano R, Ogura E, Kubo Y, Inaba A** (2003) Ethylene biosynthesis in detached young persimmon fruit is initiated in calyx and modulated by water loss from the fruit. Plant Physiol **131:** 276–286

**Nashilevitz S, Melamed-Bessudo C, Izkovich Y, Rogachev I, Osorio S, Itkin M, Adato A, Pankratov I, Hirschberg J, Fernie AR, et al** (2010) An *orange ripening* mutant links plastid NAD(P)H dehydrogenase complex activity to central and specialized metabolism during tomato fruit maturation. Plant Cell **22:** 1977–1997

**Naumann B, Busch A, Allmer J, Ostendorf E, Zeller M, Kirchhoff H, Hippler M** (2007) Comparative quantitative proteomics to investigate the remodeling of bioenergetic pathways under iron deficiency in *Chlamydomonas reinhardtii*. Proteomics **7:** 3964–3979

**Osborne TF, Espenshade PJ** (2009) Evolutionary conservation and adaptation in the mechanism that regulates SREBP action: what a long, strange tRIP it's been. Genes Dev **23:** 2578–2591

**Rawson RB, Zelenski NG, Nijhawan D, Ye J, Sakai J, Hasan MT, Chang TY, Brown MS, Goldstein JL** (1997) Complementation cloning of *S2P*, a gene encoding a putative metalloprotease required for intramembrane cleavage of SREBPs. Mol Cell **1:** 47–57

**Roca M, Hornero-Méndez D, Gandul-Rojas B, Mínguez-Mosquera MI** (2006) Stay-green phenotype slows the carotenogenic process in *Capsicum annuum* (L.) fruits. J Agric Food Chem **54:** 8782–8787

**Ronen G, Cohen M, Zamir D, Hirschberg J** (1999) Regulation of carotenoid biosynthesis during tomato fruit development: expression of the gene for lycopene epsilon-cyclase is down-regulated during ripening and is elevated in the mutant *Delta*. Plant J **17:** 341–351

**Rudner DZ, Fawcett P, Losick R** (1999) A family of membrane-embedded metalloproteases involved in regulated proteolysis of membrane-associated transcription factors. Proc Natl Acad Sci USA **96:** 14765–14770

**Schwacke R, Schneider A, van der Graaff E, Fischer K, Catoni E, Desimone M, Frommer WB, Flügge UI, Kunze R** (2003) ARAMEMNON, a novel database for Arabidopsis integral membrane proteins. Plant Physiol **131:** 16–26

**Seo PJ, Kim SG, Park CM** (2008) Membrane-bound transcription factors in plants. Trends Plant Sci **13:** 550–556

**Seymour GB, Ryder CD, Cevik V, Hammond JP, Popovich A, King GJ, Vrebalov J, Giovannoni JJ, Manning K** (2011) A *SEPALLATA* gene is involved in the development and ripening of strawberry (*Fragaria x ananassa* Duch.) fruit, a non-climacteric tissue. J Exp Bot **62:** 1179–1188

**Sink KC, Herner RC, Knowlton LL** (1974) Chlorophyll and carotenoids of the *rin* tomato mutant. Can J Bot **52:** 1657–1660

**Srivastava A, Handa AK** (2005) Hormonal regulation of tomato fruit development: a molecular perspective. J Plant Growth Regul **24:** 67–82

**Sun XW, Fu TJ, Chen N, Guo JK, Ma JF, Zou MJ, Lu CM, Zhang LX** (2010) The stromal chloroplast Deg7 protease participates in the repair of photosystem II after photoinhibition in Arabidopsis. Plant Physiol **152:** 1263–1273

**Symons GM, Davies C, Shavrukov Y, Dry IB, Reid JB, Thomas MR** (2006) Grapes on steroids: brassinosteroids are involved in grape berry ripening. Plant Physiol **140:** 150–158

**Tanksley SD, Ganal MW, Prince JP, de Vicente MC, Bonierbale MW, Broun P, Fulton TM, Giovannoni JJ, Grandillo S, Martin GB, et al** (1992) High density molecular linkage maps of the tomato and potato genomes. Genetics **132:** 1141–1160

**Timmis JN, Ayliffe MA, Huang CY, Martin W** (2004) Endosymbiotic gene transfer: organelle genomes forge eukaryotic chromosomes. Nat Rev Genet **5:** 123–135

**Vrebalov J, Pan IL, Arroyo AJM, McQuinn R, Chung M, Poole M, Rose JKC, Seymour G, Grandillo S, Giovannoni J, et al** (2009) Fleshy fruit expansion and ripening are regulated by the tomato *SHATTERPROOF* gene *TAGL1.* Plant Cell **21:** 3041–3062

**Vrebalov J, Ruezinsky D, Padmanabhan V, White R, Medrano D, Drake R, Schuch W, Giovannoni J** (2002) A *MADS*-box gene necessary for fruit ripening at the tomato *ripening-inhibitor* (*rin*) locus. Science **296:** 343–346

**Waters MT, Langdale JA** (2009) The making of a chloroplast. EMBO J **28:** 2861–2873

**Watkins CB, Nock JF, Weis SA, Jayanty S, Beaudry RM** (2004) Storage temperature, diphenylamine, and pre-storage delay effects on soft scald, soggy breakdown and bitter pit of 'Honeycrisp' apples. Postharvest Biol Technol **32:** 213–221

**Yen HC, Shelton BA, Howard LR, Lee S, Vrebalov J, Giovannoni JJ** (1997) The tomato *high-pigment* (*hp*) locus maps to chromosome 2 and influences plastome copy number and fruit quality. Theor Appl Genet **95:** 1069–1079

**Zhang M, Yuan B, Leng P** (2009) The role of ABA in triggering ethylene biosynthesis and ripening of tomato fruit. J Exp Bot **60:** 1579–1588

**Zimmermann P, Hirsch-Hoffmann M, Hennig L, Gruissem W** (2004) GENEVESTIGATOR: Arabidopsis microarray database and analysis toolbox. Plant Physiol **136:** 2621–2632